DOI: 10.1002/adsc.200700200

Palladium Catalytic Species Containing Chiral Phosphites: Towards a Discrimination between Molecular and Colloidal Catalysts

Isabelle Favier,[a] Montserrat Gómez,[a,b,*] Guillermo Muller,[a] M. Rosa Axet,[c] Sergio Castillón,[c] Carmen Claver,[c,*] Susanna Jansat,[d] Bruno Chaudret,[d,*] and Karine Philippot[d,*]

[a] Departament de Química Inorgànica, Universitat de Barcelona, Martí i Franquès, 1-11, 08028 Barcelona, Spain
[b] Laboratoire Hétérochimie Fondamentale et Appliquée, UMR CNRS 5069, 118, route de Narbonne, 31062 Toulouse cedex 9, France
Fax: (+33)-5-6155-8204; e-mail: gomez@chimie.ups-tlse.fr
[c] Departament de Química Física i Química Inorgànica i Química Analítica i Química Orgànica, Universitat Rovira i Virgili, c/Marcel·lí Domingo, s/n, 43007 Tarragona, Spain
[d] Laboratoire de Chimie de Coordination, UPR CNRS 8241, 205, route de Narbonne, 31077 Toulouse cedex 04, France

Received: April 20, 2007; Revised: July 30, 2007

Supporting information for this article is available on the WWW under http://asc.wiley-vch.de/home/.

Abstract: Palladium nanoparticles (**Pd1**–**Pd3**) stabilized by chiral diphosphite ligands (**1**–**3**), were synthesized and tested as catalysts for the allylic alkylation reaction, using different substrates (*rac*-**I**, *rac*-**III** and *rac*-**V**). Carbohydrate ligands (**1** and **2**), only differing in the C-3 configuration, led to a remarkable difference in stability of the corresponding nanoparticles: while **Pd1** is a robust catalyst, **Pd2** decomposes into molecular species. In addition, the high enantioselective systems, **Pd1** and **Pd3**, are only active for a substrate containing phenyl groups. Concerning the catalytic behaviour of the corresponding molecular systems, palladium complexes coordinated to ligands **1** or **3**, gave excellent asymmetric inductions, but an analogous catalyst accommodating ligand **2**, was not found selective.

Keywords: allylic substitution; catalyst nature; chiral phosphites; nanostructures; palladium

Introduction

An ever-increasing interest has been devoted in the past years to metal nanoparticles because of their small size and electronic configuration giving rise to interesting properties in various areas.[1] In this respect, the use of metal nanoparticles for catalytic transformations of organic substrates is a growing area.[2] Metal nanoparticles have been proved to be efficient and selective catalysts for reactions which are catalyzed by molecular complexes such as olefin hydrogenation or C–C coupling, for example, but also for reactions which are not or only poorly catalyzed by molecular species such as aromatic hydrocarbon hydrogenation.[2d,g,b] An unambiguous distinction between colloidal and true homogeneous catalysis is however often very difficult.[3] Despite impressive progresses in asymmetric catalysis,[4] only very few colloidal systems have been found to display an interesting activity, the best one being Pt(Pd)/cinchonidine for the hydrogenation of ethyl pyruvate.[5] Recently, BINAP-Pd nanoparticles were found to be an efficient catalyst for the asymmetric hydrosilylation of styrene under mild conditions, in contrast to the lack of activity showed by the related molecular system.[6]

Palladium particles also recently attracted a high interest as catalysts for C–C coupling reactions (mainly Heck and Suzuki couplings).[7] During the past years, some of us have developed the synthesis of metal nanoparticles through an organometallic approach.[2g,8]

This method leads to nearly monodispersed particles of very small size and displaying interesting surface coordination chemistry. This point can, in principle, be evidenced by spectroscopic methods such as NMR,[9] but also by the reactivity produced by the presence of ligands, like asymmetric induction in catalytic processes.

Concerning the chiral ligands, those arising from the chiral "pool" such as carbohydrate ligands display several advantages: they are readily available, highly functionalized, and may be systematically modified

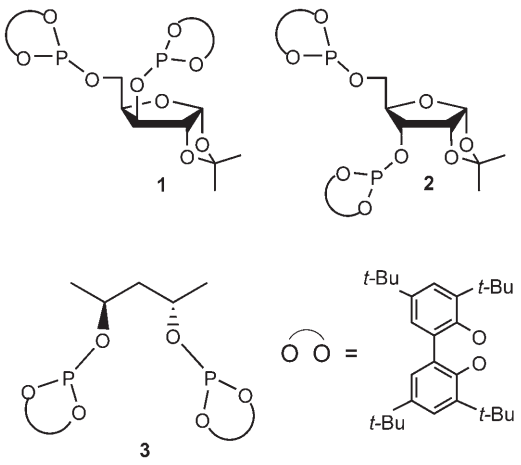

Figure 1. Chiral diphosphite ligands **1–3**.

and optical resolution is unnecessary. During the past years some of us have focused on the use of modified furanose derivatives of C_1-symmetry, as ligands in asymmetric catalysis. Some of these ligands have been successfully applied in metal-catalyzed asymmetric reactions providing excellent results in rhodium-catalyzed asymmetric hydrogenation, asymmetric hydroformylation or palladium-catalyzed asymmetric allylic substitution.[10] In particular, the use of furanoside diphosphites where the inversion of the configuration in C-3 (*xylo* or *ribo* configuration) influences strongly the catalytic behaviour, becomes especially interesting. For instance, in the rhodium-catalyzed hydroformylation of styrene the diphosphite with a *xylo* configuration, provided the same *ee* as the *ribo* diphosphite but with the opposite configuration,[11] while in the rhodium-catalyzed hydrogenation of dehydroamino acids, only the *ribo* configuration provides excellent *ee* (up to 99%).[12]

In a previous preliminary communication, we reported the asymmetric allylic alkylation of *rac*-3-acetoxy-1,3-diphenyl-1-propene with dimethyl malonate.[13] using as catalyst Pd nanoparticles stabilized by the chiral diphosphite ligand **1** (Figure 1). We observed that the nanoparticles display a high selectivity for this asymmetric process. More specifically, the reaction proceeds with one enantiomer of the racemic substrate demonstrating a very high degree of kinetic resolution. In addition, the same reaction catalyzed by the molecular species accommodating the same diphosphite ligand, under comparable conditions for matching the catalysts rates, proceeded with both enantiomers. The origin of this selectivity could be due to a particular combination between the metallic surface, the substrate and the ligand.

In order to try to understand the origin for this singular effect, we decided to carry out a comparative study using colloidal and molecular catalytic systems containing three diphosphite ligands (Figure 1), and

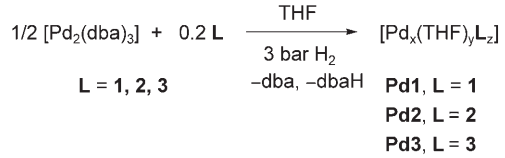

Scheme 1. Synthesis of palladium nanoparticles **Pd1–Pd3**.

employing different types of allylic substrates. Diphosphite ligand **2**, with C_1-symmetry differs from diphosphite **1** only in the configuration of C-3 of the sugar backbone, while ligand **3** differs in the flexibility of its skeleton without the bicyclic backbone. It is hoped that the various ligand/nanoparticles surface/substrate environments thus created may help to shed some light on this novel catalytic system and operating mechanism. For this purpose, we describe first the synthesis and characterization of nanoparticles and complexes containing chiral diphosphite ligands, to follow with the application of both colloids and molecular systems as catalysts in allylic alkylation of several acetate allylic substrates.

Results and Discussion

Palladium Species Containing Chiral Phosphites

Palladium Colloids

Palladium nanoparticles (colloids **Pd1–Pd3**) were synthesized from $[Pd_2(dba)_3]$ as metal precursor and the appropriate chiral diphosphite ligand,[14] **1–3** (Scheme 1). As a standard procedure, the decomposition of $[Pd_2(dba)_3]$ by H_2 (3 bars) was realized in THF inside a Fischer–Porter bottle, at room temperature and in the presence of the chosen ligand (**1–3**; Pd/**L** = 1/0.2).

The Pd nanoparticles were isolated as black powders after pentane precipitation. Transmission electron microscopy (TEM) revealed the presence of small spherical, but in some cases agglomerated, particles of *ca.* 4 nm mean size, as seen in Figure 2, Figure 3, and Figure 4. Colloids **Pd1** and **Pd2** are similar in aspect and mean sizes. These results are not very surprising since the stabilizing ligands **L1** and **L2** only differ in the configuration of carbon atom C-3 of their sugar backbones. Size histograms built from the displayed micrographs, show narrow size distributions with a majority of particles having a size corresponding to the mean one, most particularly for **Pd1**.

Colloid **Pd3** contains nanoparticles which are not well dispersed on the TEM grid in opposition to what is observed for colloids **Pd1** and **Pd2**. As a consequence of their agglomeration, the size of **Pd3** nanoparticles could not be precisely determined because of their close proximity but is estimated to be *ca.*

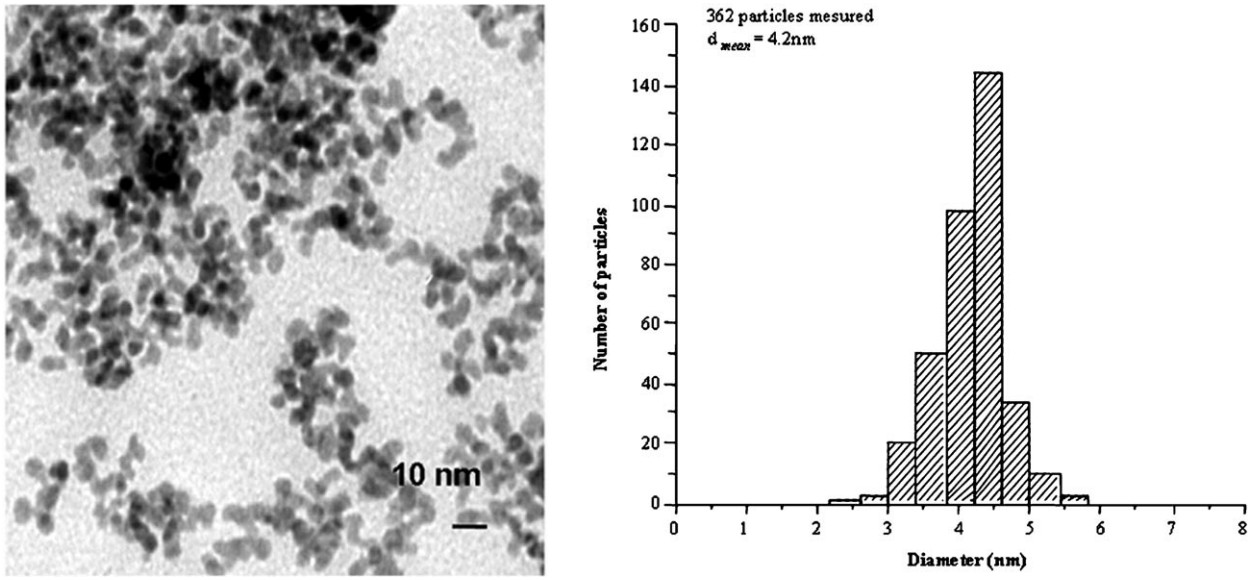

Figure 2. Transmission electron micrograph of colloid **Pd1** and the corresponding size histogram.

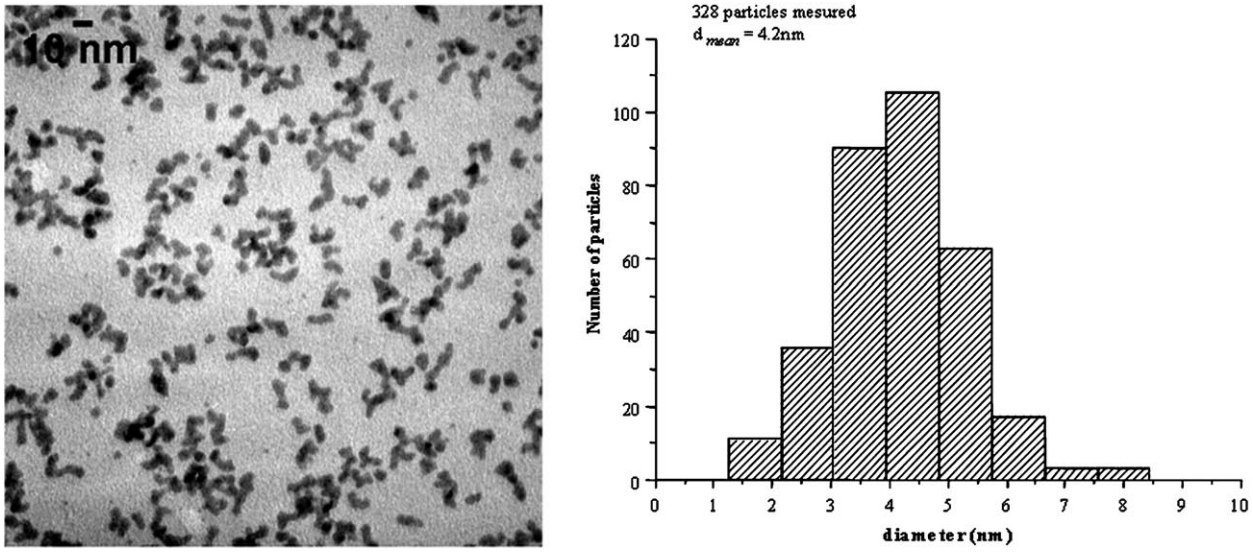

Figure 3. Transmission electron micrograph of colloid **Pd2** and the corresponding size histogram.

4 nm. This behaviour can be explained by a lower steric hindrance around the particles, since **L3** ligand shows a more flexible backbone than **L1** and **L2**.

Wide-angle X-ray scattering analyses evidenced the fcc structure of bulk palladium (Figure 5) and a coherence length which in the case of **Pd1** and **Pd3** matches the TEM observations. The small coherence length observed in the case of **Pd2** agrees with the presence of nanoparticles of irregular shape as observed on Figure 3.

Palladium Complexes

Ionic palladium complexes, **4** and **5**, containing the 1,3-diphenylallyl group were prepared from the corresponding palladium dimer and the appropriate chiral ligand, **1** and **2** respectively, in the presence of ammonium hexafluorophosphate (Scheme 2), following the methodology previously described.[15]

These compounds were obtained as monometallic complexes of general formula [Pd(η^3-1,3-$Ph_2C_3H_3$)-(L)] PF_6 (L = **1**, **2**), where L acts as a κ^2-*P,P*-bidentate ligand affording eight-membered palladacycle. Complexes **4** and **5** were fully characterized by the usual techniques. IR spectra showed strong signals at 1070

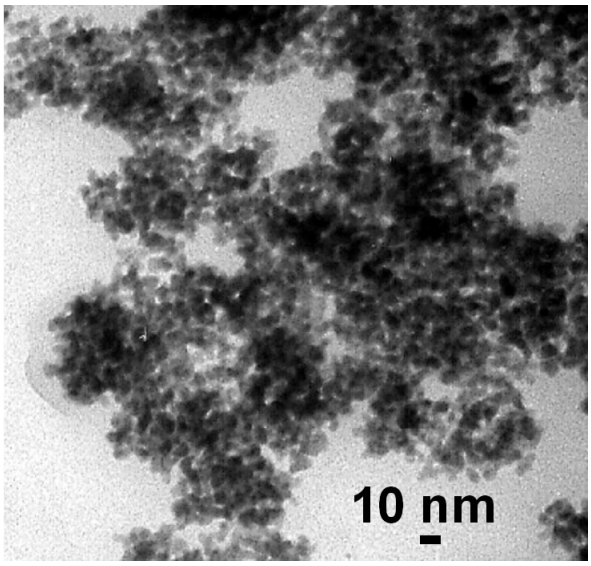

Figure 4. Transmission electron micrograph of colloid **Pd3**.

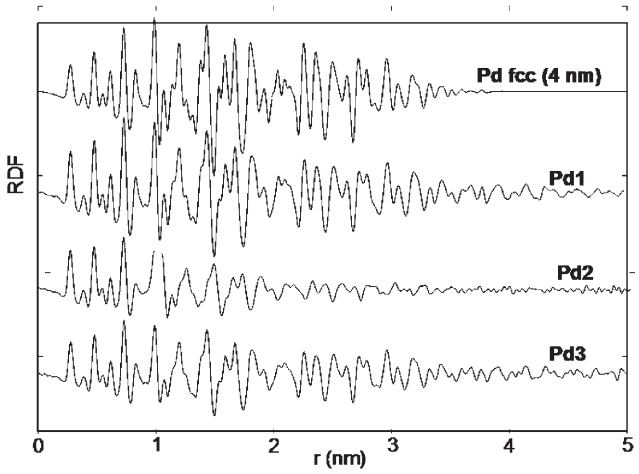

Figure 5. WAXS analysis: comparison of the rdf of colloids **Pd1**, **Pd2** and **Pd3** with a theoretical calculated for 4 nm fcc Pd nanoparticles.

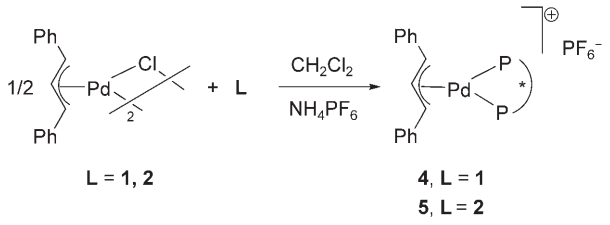

Scheme 2. Synthesis of palladium complexes **4** and **5**.

(**4**) and 1090 (**5**) cm^{-1} assigned to the P–O stretching of the phosphite moiety and at 835 (**4**) and 801 (**5**) cm^{-1} assigned to P–F stretching of the PF_6 anion. MALDI mass spectra exhibited a peak corresponding to the $[Pd(\eta^3\text{-}1,3\text{-}Ph_2C_3H_3)(L)]^+$ fragment. Unfortunately, no monocrystals of **4** or **5** could be obtained.

NMR spectroscopy allowed the structure determination of these complexes in solution. ^{31}P NMR and ^1H NMR spectra of **4** showed the presence of two species, with a ratio 2/1, invariable with the temperature (temperature range studied: 298–223 K). Both isomers are probably due to the relative position of the central allylic carbon with regard to the ligand backbone (see below). For **5**, the two isomers could not be distinguished in the temperature range analyzed (298–223 K).

We carried out a molecular modelling study of both isomers of each complex by means of semi-empirical PM3(tm) calculations (Figure 6). The two isomers result from the relative position of the central allylic carbon and the acetal group: *exo*, if both groups point to the same direction, *endo*, if they point to opposite sides. It is important to notice that the two different metallacycle arrangements were observed for the two complexes. For **4**, the palladium, two phosphorus and two oxygen atoms are quasi coplanar, while for **5**, the metallacycle shows an eight-member crown conformation. These distinct conformations lead to a different steric hindrance of the biphenyl *tert*-butyl groups towards the 1,3-diphenylallyl moiety. As a result, the two terminal allyl carbon atoms are electronically well differentiated for **4**, as observed by the calculated distances [Δ(Pd–C) = 0.02 and 0.023 Å for *endo* and *exo* isomers, respectively], while for **5**, no important variations are produced [Δ(Pd–C) = 0.003 and 0.004 Å for *endo* and *exo* isomers, respectively]. These data are in agreement with the remarkable differences in the asymmetric induction observed in Pd-catalyzed allylic alkylation using *rac*-3-acetoxy-1,3-diphenyl-1-propene (*rac*-**I**) as substrate (see below).

For the analogous complex coordinated to ligand **3**, the corresponding allyl complex, $[Pd(\eta^2\text{-}1,3\text{-}Ph_2\text{-}C_3H_3)(\kappa^2\text{-}P,P\text{-}\mathbf{3})]^+$, has been also calculated. In this case only one allylic structure is possible, due to the steric hindrance of the ligand (Figure 7 a).

Enantioselective Allylic Alkylation

Asymmetric allylic alkylation of racemic substrates *rac*-3-acetoxy-1,3-diphenyl-1-propene (*rac*-**I**) and *rac*-3-acetoxy-1-cyclohexene (*rac*-**III**) with dimethyl malonate under basic Trost conditions,[16] was carried out using Pd catalytic systems containing ligands **1–3** (Scheme 3).

Two types of catalytic precursors were employed, molecular systems generated *in situ* from $[Pd(\mu\text{-}Cl)(\eta^3\text{-}C_3H_5)]_2$ and the appropriate ligand (Pd/L = 1/1.25), and colloidal ones, using pre-formed palladium nanoparticles (see above). These results are summarized in Table 1, Table 2 and Table 3 for *rac*-**I** and in Table 5 for *rac*-**III**.

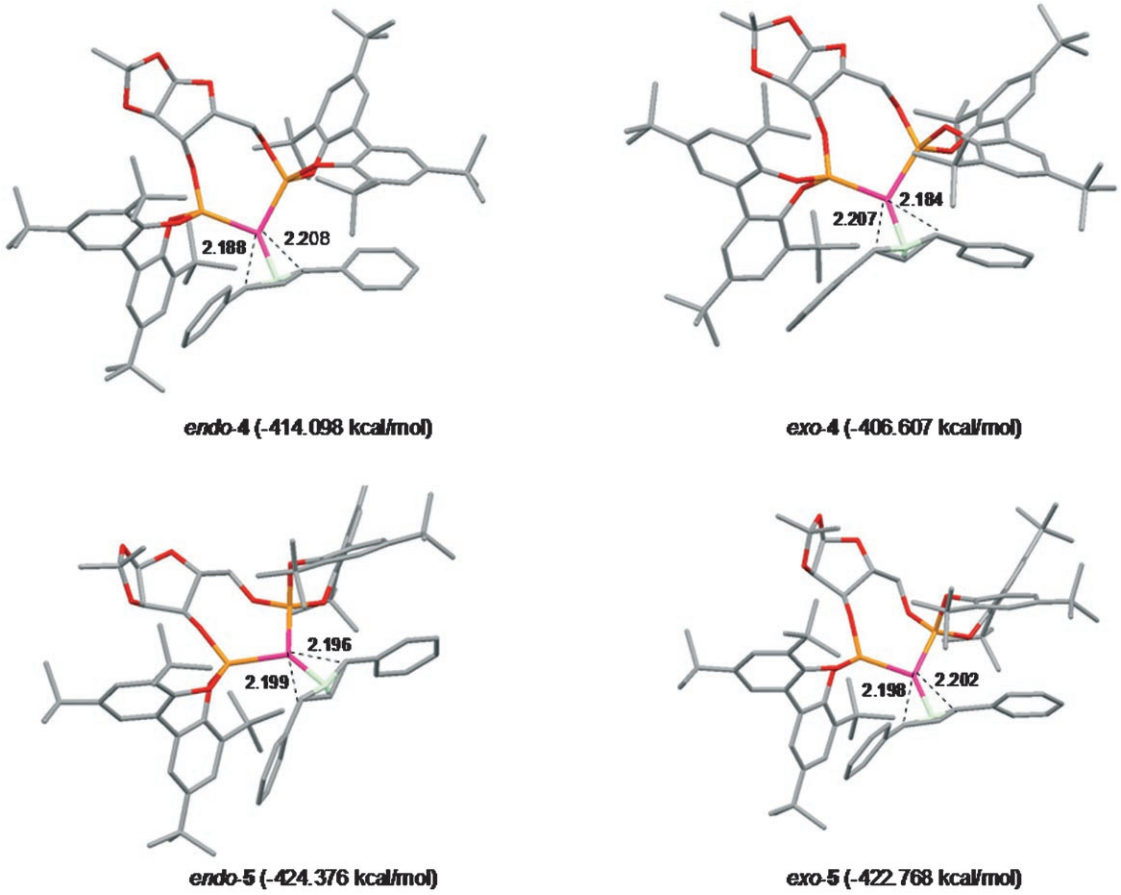

Figure 6. Calculated structures [PM3 (tm)] for cationic species of complexes **4** and **5** (in parenthesis their relative formation enthalpies). Hydrogen atoms are omitted for clarity. Pd–C bond distances are in Å.

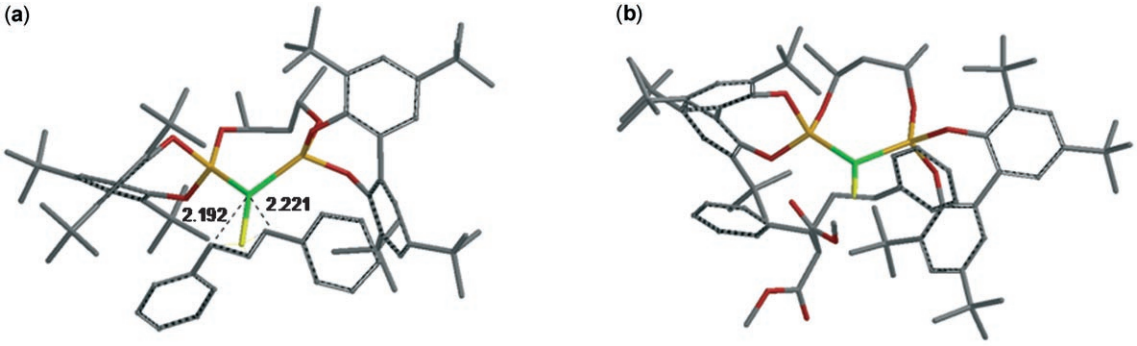

Figure 7. Modelled structures [PM3 (tm)] for palladium complexes containing ligand **3**: cationic palladium allyl complex, $[Pd(\eta^2\text{-}1,3\text{-}Ph_2\text{-}C_3H_3)(\kappa^2\text{-}P,P\text{-}\mathbf{3})]^+$ (**a**); neutral palladium olefin complex, $[Pd(\eta^2\text{-}\{Ph\text{-}CH{=}CH\text{-}CH(Ph)(CH(COOMe)_2\}(\kappa^2\text{-}P,P\text{-}\mathbf{3})]$ (**b**). Hydrogen atoms are omitted for clarity. Pd–C bond distances are in Å.

Pd-Catalyzed Allylic Alkylation of *rac*-3-Acetoxy-1,3-diphenyl-1-propene (*rac*-I)

Molecular Catalytic Precursors

The three Pd/**L** catalytic systems (**L** = **1**–**3**) were active in the allylic alkylation of *rac*-**I**. The highest activity and enantioselectivity were observed for Pd/**3** containing the open alkyl chain (entry 3 versus 1 and 2, Table 1). Concerning the catalytic systems containing carbohydrate ligands **1** and **2**, it is important to note the crucial effect of the configuration at C-3 stereocentre: while Pd/**1** gave an excellent enantioselectivity (*ee* = 90 % (*S*)), Pd/**2** led to a racemic mixture of **II** (entries 1 and 2, Table 1).

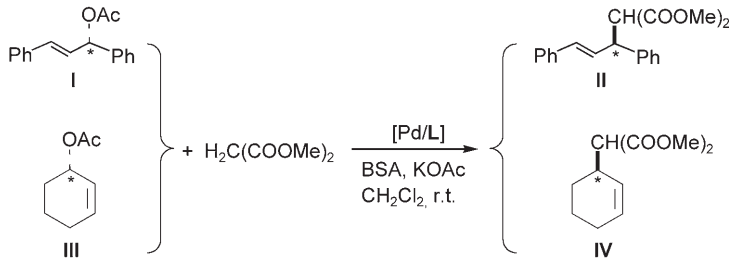

Scheme 3. Allylic alkylation of *rac*-**I** and *rac*-**III** using Pd/**L** catalytic systems (**L** = **1–3**).

Table 1. Asymmetric allylic alkylation of *rac*-**I** catalyzed by molecular palladium systems containing chiral ligands **1–3**.[a]

Entry	**L**	Time [h]	Conversion [%][b]	*ee* **I** [%][c]	*ee* **II** [%][c]
1[d]	**1**	1.5	83	0	90 (*S*)
2	**2**	1.5	80	0	0
3	**3**	0.15	100	-	94 (*S*)

[a] Results from duplicated experiments; Pd/*rac*-**I**/dimethyl malonate/BSA = 1/100/300/300. See Scheme 3.
[b] Conversions based on the substrate **I** and determined by ^{1}H NMR.
[c] Determined by HPLC on a Chiralcel-OD column. Absolute configuration of **II** in parentheses, determined by optical rotation: U. Leutenegger, G. Umbricht, C. Fahrni, P. V. Matt, A. Pfaltz, *Tetrahedron* **1992**, *48*, 2143-2156.
[d] See ref.[13]

This fact can be explained by the electronic differentiation produced at the terminal allylic carbon atoms in the Pd allylic intermediates, complexes **4** and **5** (see above). Therefore, the metallacycle formed in the case of **4** induces a significant electronic differentiation between both terminal allylic carbon atoms, in contrast to the lack of effect induced by **5** (see relative Pd–C bond distances in Figure 6). Comparing Pd/**1** and Pd/**3** catalytic systems (entries 1 and 3, Table 1), we observe that the asymmetric induction was excellent in both cases but the activity was significantly superior for Pd/**3**, which contains a ligand with a flexible backbone. The calculated structures for intermediates containing ligand **3** allow to justify the high enantioselectivity observed. Concerning its palladium allyl intermediate, only one stable isomer is possible due to the pocket environment formed upon coordination of the palladium to ligand **3**, leading to a significant electronic differentiation between both terminal allylic carbon atoms (Pd–C calculated distances are 2.192 and 2.221 Å, Figure 7 a). Moreover, the nucleophile attacks preferentially the more electrophilic terminal allylic carbon atom, because the attack on the other atom is blocked by the steric hindrance produced in the resulting Pd(0) intermediate (Figure 7 b).

Table 2. Asymmetric allylic alkylation of *rac*-**I** catalyzed by colloidal palladium systems, **Pd1**–**Pd3**.[a]

Entry	**PdL/L**	Time [h]	Conversion [%][b]	*ee* **I** [%][c]	*ee* **II** [%][c]	$k_{(R)\text{-}\mathbf{I}}/k_{(S)\text{-}\mathbf{I}}$[d]
1[e]	**Pd1/-**	168	0	-	-	-
2[e]	**Pd1/1**	10	50	70 (*S*)	96 (*S*)	11.6
3[e]	**Pd1/1**	24	56	89 (*S*)	97 (*S*)	16.4
4	**Pd2/-**	168	0	-	-	-
5	**Pd2/2**	24	0	-	-	-
6	**Pd2/2**	48	100	-	11 (*S*)	-
7	**Pd3/-**	168	0	-	-	-
8	**Pd3/3**	3	68	94 (*S*)	92 (*S*)	8.3
9	**Pd3/3**	24	88	>99 (*S*)	90 (*S*)	4.7
10	**Pd1/2**	24	0	0	-	-
11	**Pd2/1**	24	100	-	89 (*S*)	-

[a] Results from duplicated experiments; Pd/*rac*-**I**/dimethyl malonate/BSA = 1/100/300/300. Pd/Lstabilizer/Lfree ligand = 1/0.2/1.05.
[b] Conversions based on the substrate **I** and determined by ^{1}H NMR.
[c] Determined by HPLC on a Chiralcel-OD column. Absolute configuration of **II** in parentheses, determined by optical rotation: U. Leutenegger, G. Umbricht, C. Fahrni, P. V. Matt, A. Pfaltz, *Tetrahedron* **1992**, *48*, 2143-2156.
[d] Calculated from $k_R/k_S = \ln[(1-C/100)(1-ee/100)]/\ln[(1-C/100)(1+ee/100)]$ (C. H. Chen, Y. Fujimoto, G. Girdaukas, C. J. Sih, *J. Am. Chem. Soc.* **1982**, *105*, 7294-7299).
[e] See ref.[13]

Table 3. Asymmetric allylic alkylation of *rac*-**I** catalyzed by molecular palladium systems containing chiral ligands **1** and **3**, at different Pd concentrations.[a]

Entry	L	Pd/**I**	Time [h]	Conversion [%][b]	*ee* **I** [%][c]	*ee* **II** [%][c]	$k_{(R)\text{-}\mathbf{I}}/k_{(S)\text{-}\mathbf{I}}$[d]
1[e]	**1**	1/100	1.5	83	0	90 (*S*)	1
2[e]	**1**	1/2,000	3	43	26 (*S*)	90 (*S*)	2.6
3[e]	**1**	1/10,000	24	72	43 (*S*)	90 (*S*)	2.0
4	**3**	1/100	0.15	100	-	94 (*S*)	-
5	**3**	1/2,500	0.5	88	>99 (*S*)	91 (*S*)	4.7

[a] Results from duplicated experiments; *rac*-**I**/dimethyl malonate/BSA = 1/3/3.
[b] Conversions based on the substrate **I** and determined by ^{1}H NMR.
[c] Determined by HPLC on a Chiralcel-OD column. Absolute configuration of **II** in parentheses, determined by optical rotation: U. Leutenegger, G. Umbricht, C. Fahrni, P. V. Matt, A. Pfaltz, *Tetrahedron* **1992**, *48*, 2143-2156.
[d] Calculated from $k_R/k_S = \ln[(1-C/100)(1-ee/100)]/\ln[(1-C/100)(1+ee/100)]$ (C. H. Chen, Y. Fujimoto, G. Girdaukas, C. J. Sih, *J. Am. Chem. Soc.* **1982**, *105*, 7294-7299).
[e] See ref.[13]

Table 4. Asymmetric allylic alkylation of *rac*-**V** catalyzed by colloidal and molecular palladium systems containing chiral ligands **1** and **2**.[a]

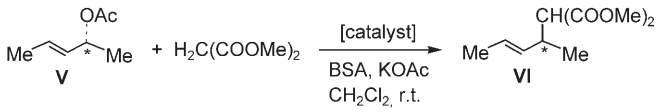

Entry	Catalyst (precursor)	Time [h]	Conversion [%][b]	*ee* **VI** [%][c]
1	**Pd1**/**1** (colloidal)	24	0	-
2	Pd/**1** (molecular)	3	45	50 (*R*)
3	**Pd2**/**2** (colloidal)	72	82	0
4	Pd/**2** (molecular)	7	80	0

[a] Results from duplicated experiments; Pd/*rac*-**V**/dimethyl malonate/BSA = 1/100/300/300. For colloidal systems, Pd/Lstabilizer/Lfree ligand = 1/0.2/1.05.
[b] Conversions based on the substrate **V** and determined by ^{1}H NMR.
[c] Determined by optical rotation. Absolute configuration of **VI** in parentheses, determined by optical rotation: L. Xiao, W. Weissensteiner, K. Mereiter, M. Widhalm, *J. Org. Chem.* **2002**, *67*, 2206-2214.

Colloidal Catalytic Precursors

When *rac*-**I** reacted with dimethyl malonate using colloids **Pd1**, **Pd2** and **Pd3** as catalysts, no reaction was observed (entries 1, 4, 7, Table 2). However, catalysts **Pd1** and **Pd3** became active after addition of 1 equivalent of the corresponding ligand in the catalytic reaction mixture (entries 2 and 9, Table 2). This fact can be related to the presence of free ligand in solution which prevents nanoparticles agglomeration and/or leaching of palladium.

Colloids **Pd1** and **Pd3**, similarly to the corresponding molecular systems, showed excellent enantioselectivities (see Table 1). However, in contrast to the molecular catalysts, **Pd1** and **Pd3** catalytic systems provided an excellent kinetic resolution (entries 3 and 8 of Table 2 *versus* entries 1 and 3 of Table 1). The kinetic resolution of the racemic substrate using **Pd1** ($k_{(R)\text{-}\mathbf{I}}/k_{(S)\text{-}\mathbf{I}} \approx 16$; entry 3, Table 2) is better than that using **Pd3** ($k_{(R)\text{-}\mathbf{I}}/k_{(S)\text{-}\mathbf{I}} \approx 5$; entry 9, Table 2), since for **Pd1** the reaction practically stops after 55% conversion,[13] while for **Pd3** the reaction slowly evolves with the time.

Looking for information about the origin of this kinetic resolution, the reaction of *rac*-**I** with dimethyl malonate was carried out with the molecular system at different Pd concentrations (Table 3). Colloid **Pd1** behaves differently than the corresponding molecular system Pd/**1** (entries 2 and 3, Table 2, *versus* entries 1–3, Table 3), since for **Pd1** the reaction practically stops after 10 h. In addition, the allylic alkylation of enriched substrate **I** [(*S*)-**I**/(*R*)-**I** = 92/8] was studied using the colloidal system **Pd1** and also the very dilute molecular catalytic system (Pd/**1** = 1/10,000).[13] After 30 h, only 10% of enriched substrate was converted in the colloidal case, but *ca.* 70% in the molecular one, giving the alkylated product **II** in 95% *ee* in both cases. This fact shows that for the colloidal catalyst, almost only (*R*)-**I** leads to the formation of the alkylation product.

In contrast, for **Pd3** and Pd/**3** no kinetic differences were observed between molecular and colloidal systems (entry 5, Table 3, *versus* entry, 9 Table 2). Therefore for this system, the high activity and selectivity showed by both molecular (entries 4 and 5, Table 3) and colloidal (entries 8 and 9, Table 2) catalysts, do not provide any evidence about the nature of the catalyst.

Concerning **Pd2** (entries 5 and 6, Table 2), activity was only observed at long reaction times (more than 24 h), probably due to some decomposition giving molecular species.

In order to corroborate the robustness of colloidal **Pd1** under catalytic conditions, free ligand **2** (and no **1**) was added to the catalytic reaction mixture (ratio Pd/**1**/**2** = 1/0.2/1.05). In this case the catalyst was total-

Table 5. Asymmetric allylic alkylation of *rac*-**III** catalyzed by molecular and colloidal palladium systems containing chiral ligands **1** and **3**.[a]

Entry	L	Pd/**III**	Time [h]	Conversion [%][a]	*ee* **III** (%)[a]	*ee* **IV** [%][a]	$k_{(S)\text{-III}}/k_{(R)\text{-III}}$[b]
				Molecular systems[c]			
1	**1**	1/100	0.5	100	-	22 (*S*)	-
2	**1**	1/5,000	24	19	28 (*R*)	27 (*S*)	14.0
3	**3**	1/100	0.25	48	>98 (*R*)	88 (*S*)	156.5
4	**3**	1/100	0.5	73	>98 (*R*)	73 (*S*)	8.3
5	**3**	1/5,000	24	5	0	nd[d]	-
				Colloidal systems[e]			
6	**1**	1/100	24	0	0	-	-
7	**3**	1/100	24	7	0	nd[d]	-

[a] Conversions based on the substrate **III.** Both conversions and enantioselectivities were determined by GC. Absolute configuration of **IV** in parentheses, determined by optical rotation: L. Xiao, W. Weissensteiner, K. Mereiter, M. Widhalm, *J. Org. Chem.* **2002**, *67*, 2206-2214.

[b] Calculated from $k_R/k_S = \ln[(1-C/100)(1-ee/100)]/\ln[(1-C/100)(1+ee/100)]$ (C. H. Chen, Y. Fujimoto, G. Girdaukas, C. J. Sih, *J. Am. Chem. Soc.* **1982**, *105*, 7294-7299).

[c] Results from duplicated experiments; *rac*-**III**/dimethyl malonate/BSA = 1/3/3. See Scheme 3.

[d] Not determined.

[e] Results from duplicated experiments; *rac*-**III**/dimethyl malonate/BSA = 1/3/3. Pd/Lstabilizer/Lfree ligand = 1/0.2/1.05. See Scheme 3.

ly inactive (entry 10, Table 2), analogously to the system without free ligand added (entry 1). Probably, ligand **2** does not interact with **Pd1** nanoparticles. And what is more important, **Pd1** does not leach molecular species. On the contrary, the "cross-system" formed by **Pd2** nanoparticles and free ligand **1**, exhibits a high activity and enantioselectivity (entry 11, Table 2), similar to that observed for molecular system Pd/**1** (entry 1, Table 1), pointing to the decomposition of **Pd2** nanoparticles to give molecular species, mainly molecular Pd/**1** species due to the relative ratio of both ligands (**1**/**2** = 1.05/0.2). The same trend between palladium systems containing **1** and **2** was also found using *rac*-3-acetoxy-1,3-dimethyl-1-propene (*rac*-**V**) as substrate (Table 4). The colloidal **Pd1** catalyst was found inactive, in contrast to the molecular system (entry 1 versus 2, Table 4). However a similar reactivity was observed for both molecular and colloidal catalytic systems involving ligand **2**. Again, the activity and selectivity observed for Pd/**2** molecular system was analogous to that observed for colloidal catalyst (entries 3 and 4, Table 4), demonstrating definitively the formation of molecular species from colloid **Pd2**.

In order to shed more light concerning the interaction between the metallic surface and the substrate, the cyclic racemic substrate, 3-acetoxy-1-cyclohexene, has been considered.

Pd-Catalyzed Allylic Alkylation of *rac*-3-Acetoxy-1-cyclohexene (*rac*-III)

The asymmetric allylic alkylation of the cyclic substrate *rac*-**III** with colloids **Pd1** and **Pd3** was carried out (Scheme 3, Table 5). Concerning the molecular systems, Pd/**3** was more selective than Pd/**1**, giving **IV** with *ee* up to 88% (entry 1 versus entry 3, Table 5). The high enantioselectivity observed for Pd/**3** is probably due to the more important steric hindrance of the ligand **3** towards the allyl moiety than that of ligand **1** (see structures for allyl complexes containing 1,3-diphenyl allyl, Figure 6 and 7), due to the pocket environment around the "Pd-allyl" moiety.

But what is more remarkable is the high kinetic resolution resulting with the Pd/**3** catalytic system. The substrate (*S*)-**III** was resolved more than 150 times faster than its enantiomer at *ca.* 50% conversion (entry 3, Table 5).

When the palladium content was low (Pd/substrate = 1/5,000), both Pd/**1** and Pd/**3** systems were not very active, giving 19 and 5% conversion after 24 h, respectively (entries 2 and 5, Table 5).

With regard to colloidal systems, both **Pd1** and **Pd3** exhibited a negligible activity at long reaction time (entries 6 and 7, Table 5), showing both their stability under the catalytic conditions used and the low affinity for alkyl substrates, in contrast to the behaviour observed for the allylic alkylation of *rac*-**I** (entries 3 and 9, Table 2). In addition, these colloidal systems do not give palladium leaching, independently of the substrate used and confirming their robustness.

Conclusions

We report in this paper, novel asymmetric catalytic systems based on palladium nanoparticles. These systems where found to be dependent both upon the ligands and the substrates in a much more dramatic way than corresponding molecular systems. We find that small modifications in carbohydrate phosphite derivatives lead to important differences in selectivity. Therefore, chiral diphosphites, **1** and **2**, which only differ at C-3 configuration of the carbohydrate backbone, exhibit dramatic differences in their catalytic behaviour. While Pd/**1** molecular system is highly enantioselective ($ee = 90\%$ for the allylic alkylation of *rac*-**I**), the analogous Pd/**2** system does not induce any selectivity ($ee = 0\%$ for the same reaction). This fact is in agreement with the modelling of palladium allylic intermediates (compounds **4** and **5**), showing that upon coordination to palladium, ligand **1** causes an efficient electronic discrimination between both terminal allylic carbon atoms, in contrast to the symmetrical environment produced by **2**. In addition, palladium nanoparticles stabilized with these ligands (**Pd1** and **Pd2**) show a remarkable difference of stability. Under catalytic conditions using *rac*-**I** or *rac*-**V** as substrates, **Pd2** decomposes into molecular species, whereas **Pd1** does not.

When the carbohydrate skeleton is substituted by the flexible alkyl 2,4-dimethylpentyl backbone (ligand **3**) high activity and excellent selectivity are observed when molecular catalytic precursor is used (for allylic alkylation of both *rac*-**I** and *rac*-**III**), mainly for the less hindered substrate, cyclohexenyl derivative *rac*-**III**, reaching an enantiomeric excess up to 88%. The excellent enantioselectivity observed in both alkylated products, **II** and **IV**, can be explained by the pocket effect of the ligand upon coordination to the metal, as stated by modelling studies of palladium intermediates containing both 1,3-diphenyl and cyclohexenyl allyl moieties. Concerning the palladium nanoparticles stabilized by **3**, **Pd3** is a highly active and selective system for the allylic alkylation of *rac*-**I** in a similar way as the molecular catalytic system. But, in contrast to the molecular catalyst, it is almost inactive for the alkylation of *rac*-**III**.

It is also noteworthy the excellent kinetic resolution showed by **Pd1** in the allylic alkylation of *rac*-**I**, which has not been observed using **Pd2**. This fact points to a key-lock matching between substrate and catalyst.

From the point of view of the substrate using stable colloidal catalysts (**Pd1** and **Pd3**), alkyl-substituted allyl acetates (*rac*-**III** and *rac*-**V**) are not alkylated, while the phenylallyl acetate (*rac*-**I**) is. This fact is in agreement with the strong preference shown by metallic surfaces for aryl groups, probably due to π-coordination between the metallic surface and the aromatic group whereas alkyl groups can only lead to weak agostic interactions. Therefore, aryl-substituted allyl substrates could be envisaged as substrate models to distinguish molecular from colloidal catalysts.

In summary this study demonstrates that : i) catalysis by nanoparticles may be very effective in terms of enantioselectivity; ii) the system is much more sensitive to the adjustment between the metal, the ligand and the substrate than the corresponding molecular catalysts, in a way which may resemble enzymatic systems. This may explain the very limited number of enantioselective catalytic systems which involved nanoparticles. Further studies in this field will have to integrate the necessity of this tuning if one wants to exploit the tremendous potential of these new catalytic systems.

Experimental Section

General Remarks

All compounds were prepared under a purified nitrogen atmosphere using standard Schlenk and vacuum-line techniques. The solvents were purified by standard procedures and distilled under nitrogen. $[Pd(\eta^3\text{-}C_3H_5)(\mu\text{-}Cl)]_2$,[17] $[Pd(\eta^3\text{-}1,3\text{-}Ph_2\text{-}C_3H_3)(\mu\text{-}Cl)]_2$[15a] and ligands **1**–**3**[14] were prepared as previously described. NMR spectra were recorded on Bruker DRX 500 (^1H, standard $SiMe_4$), Varian Gemini (^{13}C, 50 MHz, standard $SiMe_4$) and Bruker DRX 250 (^{31}P, 101.2 MHz, standard H_3PO_4) spectrometers in $CDCl_3$ unless otherwise cited. Chemical shifts were reported downfield from standards. IR spectra were recorded on an FT-IR Nicolet Impact 400 spectrometer. MALDI mass chromatograms were obtained on a Fisons V6-Quattro instrument using dithranol as a matrix. Enantiomeric excess were determined by HPLC on a Hewlettt–Packard 1050 Series chromatograph (Chiralcel-OD chiral column) with a UV detector, and by GC on a Hewlett–Packard 5890 Series II gas chromatograph (25 m FS-cyclodex-β-I/P column: heptakis(2,3,6-tri-*O*-methyl)-β-cyclodextrin/polysiloxane) with an FID detector. Optical rotations were measured in a Perkin–Elmer 241MC polarimeter. Elemental analyses were carried out by the "Serveis Cientifico-Tècnics" of the Universitat Rovira i Virgili in an Eager 1108 microanalyzer, by the "Service d'Analyses du LCC" in Toulouse and by the "Service Central d'Analyses du CNRS" in Lyon for phosphorus and palladium determinations. Samples for TEM analysis were prepared in a glove-box by slow evaporation of a drop of each crude colloidal solution deposited onto a holey carbon-covered copper grid. The TEM experiments were performed at the "Service Commun de Microscopie Electronique de l'Université Paul Sabatier" (TEMSCAN) on a JEOL 200 CX-T electron microscope operating at 200 kV with a point resolution of 4.5 Å and at the "Centre de microscopie électronique appliquée à la Biologie de l'Université Paul Sabatier" on a Philips CM12 electron microscope operating at 120 kV with a resolution point of 5 Å. The approximation of the particle mean size was made through a manual analysis of enlarged micrographs by measuring a number of particles on a given grid. For wide-angle X-ray scattering samples (analysis performed at the CEMES-

CNRS, Toulouse), samples were sealed in 1-mm diameter Lindemann glass capillaries. Modelling studies have been carried out using the following software: MACSPARTAN PRO Version 1.0.4. WaveFunction, Inc. 18401 Von Karman Avenue, suite 370. Irvine, CA 92612 U.S.A.

Synthesis of Complexes 4 and 5

In a purged Schlenk tube, 20 mg (0.03 mmol) of $[Pd(\eta^3\text{-}1,3\text{-}Ph_2\text{-}C_3H_3)Cl]_2$ and 63 mg (0.06 mmol) of ligand (**5** or **6**) were dissolved in 10 cm^3 of freshly distilled dichloromethane. The yellow solution was stirred for 30 min at room temperature and 28 mg of NH_4PF_6 (0.23 mmol) dissolved in 1 cm^3 of dichloromethane was then added. After 1 hour of stirring, washings with degassed water were carried out (4×5 cm^3). The organic phase was dried over anhydrous Na_2SO_4, filtered off and the solvent removed under reduced pressure. The yellow solid obtained was washed with diethyl ether (3×5 cm^3) and dried under reduced pressure. Yield of **4**: 81.6 mg (90%); yield of **5**: 77.1 mg (85%). Anal. calcd. for $C_{79}H_{105}F_6P_3O_9Pd$: C 62.76, H 6.95%; found for **4**: C 62.05, H 7.10%; found for **5**: C 62.45, H 6.80%. IR (KBr): for **4**: $\nu=$ 1070 (st, P–O), 835 (st, P–F) cm^{-1}; for **5**: $\nu=1090$ (st, P–O), 801 (st, P–F) cm^{-1}. MS (MALDI positive): $m/z=1365.6$ ($[M-PF_6]^+$) for both complexes. ^{31}P NMR ($CDCl_3$, 101.3 MHz, 298 K) for **4**: major species $\delta=129.6$ (d, 190.7 Hz) and 128.2 (d, 190.7 Hz); minor species $\delta=128.7$ (d, 190.7 Hz) and 126.9 (d, 199.2 Hz); for **5**: $\delta=125.5$ (d, 196.9 Hz) and 121.8 (d, 196.9 Hz).

General Procedure for the Synthesis of Pd Colloids

In a standard procedure, 160 mg of $[Pd_2(dba)_3]$ (0.175 mmol) were dissolved under argon at -110 °C (ethanol/N_2 bath) and under vigorous magnetic stirring in a solution of 160 mL of THF containing 0.2 equivs./Pd of the chosen ligand in a Fischer–Porter bottle. The mixture was then pressurized under dihydrogen (3 bars) at room temperature. The colour of the solution turned from purple to black in a few minutes. The vigorous stirring and the dihydrogen pressure were maintained for 18 h at room temperature, leading to black and homogeneous colloidal solutions. After depressurization, a drop of each colloidal solution was deposited under argon on a holey carbon-covered copper grid for TEM analysis. The colloidal solution was then concentrated to *ca.* 5 mL. Addition of cold pentane allowed the precipitation of the particles as black solids which were washed with pentane (2×40 mL) and dried under vacuum. The colloids were characterized by TEM analysis, elemental analysis and WAXS. Size histograms could not be built for colloid Pd3 because of the close proximity of the particles.

***Colloid* Pd1** was synthesized according to the standard procedure from 160 mg of $[Pd_2(dba)_3]$ (0.175 mmol) and 74.7 mg of diphosphite **1** (0.070 mmol). TEM: mean size 4.2 nm; eemental analysis: 81.72% Pd, 0.17% P, 14.68% C, 0.94% H.

***Colloid* Pd2** was synthesizd according to the standard procedure from 160 mg of $[Pd_2(dba)_3]$ (0.175 mmol) and 74.7 mg of diphosphite **2** (0.070 mmol). TEM: mean size 4.2 nm; elemental analysis: 72.97% Pd, 0.37% P, 13.99% C, 0.38% H.

***Colloid* Pd3** was synthesized according to the standard procedure from 160 mg of $[Pd_2(dba)_3]$ (0.175 mmol) and 62.6 mg of diphosphite **3** (0.070 mmol). TEM: mean size around 4 nm; elemental analysis: 71.75% Pd, 0.46% P, 11.78% C, 0.13% H.

General Procedure for Palladium-Catalyzed Allylic Alkylation

***Allylic alkylation of rac-3-acetoxy-1,3-diphenyl-1-propene* (I)**: For molecular catalytic systems containing ligands **1–3**, the catalytic precursor was generated *in situ* from $[Pd(\eta^3\text{-}C_3H_5)Cl]_2$ and the appropriate ligand (0.02 mmol of Pd and 0.025 mmol of chiral ligand) dissolved in 2 cm^3 of CH_2Cl_2 and stirred for 30 min before adding the substrate. For colloidal catalytic systems, 2.5 mg of preformed nanoparticles, **Pd1**–0**Pd3**, with 0.005 mmol of the appropriate ligand (for **1** and **2**: 5.2 mg; for **3**: 4.7 mg) were dissolved in 4 cm^3 of CH_2Cl_2 for 30 min before adding the substrate. *rac*-3-acetoxy-1,3-diphenyl-1-propene (252 mg, 1 mmol), dissolved in CH_2Cl_2 (2 cm^3), was then added to the catalyst solution followed by dimethyl malonate (396 mg, 3 mmols), BSA (610 mg, 3 mmols), and a catalytic amount of KOAc. The mixture was stirred at room temperature until total conversion of substrate (monitored by TLC). Then, the solution was diluted with diethyl ether, filtered over celite, and washed with saturated ammonium chloride solution ($4\times$ 10 cm^3) and water (4×10 cm^3). The organic phase was dried over anhydrous Na_2SO_4, filtered off, and solvent removed under reduced pressure. Conversions were determined by ^1H NMR and enantiomeric excesses determined by HPLC on a Chiralcel OD column, using hexane/2-propanol, 99/1, as eluent, in a flow of 0.3 cm^3min^{-1}.

***Allylic alkylation of rac-3-acetoxy-1-cyclohexene* (III)**: The procedure was analogous to the one described for the *rac*-3-acetoxy-1,3-diphenyl-1-propene. Conversions were determined by ^1H NMR and enantiomeric excesses were determined by GC on a FS-cyclodex-β-I/P column.

***Allylic alkylation of rac-3-acetoxy-1,3-dimethyl-1-propene* (V)**: The procedure was analogous to the one described for the *rac*-3-acetoxy-1,3-diphenyl-1-propene. Conversions were determined by ^1H NMR and enantiomeric excesses were determined by polarimetry.

Acknowledgements

The authors thank Ministerio de Educación y Ciencia (CTQ2004–01546/BQU, CTQ2004–04412/BQU and CTQ2005–03124, Consolider Ingenio 2010, CSD2006–0003), Generalitat de Catalunya (2005SGR007777), CNRS (PICS N°2428) and Région Midi-Pyrénées (CTP N°03007519) for financial support, and Pierre Lecante (CEMES-CNRS) for WAXS analysis. M.R.A. thanks Fons Social Europeu for a predoctoral grant.

References

[1] a) *Nanoscale Materials in Chemistry*, (Ed.: K. J. Blabunde), Wiley-Interscience, New York, **2001**; b) *Metal Nanoparticles: Synthesis Characterization and Applications*, (Eds.: D. L. Feldheim, C. A. Foss Jr), Marcel

Dekker, New York, **2002**; c) *Nanoparticles. From theory to application*, (Ed.: G. Schmid), Wiley-VCH, Weinheim, **2004**.

[2] a) J. D. Aiken III, R. G. Finke, *J. Mol. Catal. A: Chemical A* **1999**, *145*, 1–44; b) M. A. El-Sayed, *Acc. Chem. Res.* **2001**, *34*, 257–264; c) H. Bönnemann, R. M. Richards, *Eur. J. Inorg. Chem.* **2001**, 2455–2480; d) A. Roucoux, J. Schulz, H. Patin, *Chem. Rev.* **2002**, *102*, 3757–3778; e) J. Dupont, G. S. Fonseca, A. P. Umpierre, P. F. P. Fichtner, S. R. Teixeira, *J. Am. Chem. Soc.* **2002**, *124*, 4228–4229; f) A. Roucoux, K. Philippot, *Hydrogenation with noble metal nanoparticles*, in: *Handbook of Homogenous Hydrogenations*, (Ed.: G. de Vries), Wiley-VCH, Weinheim, **2006**; g) S. Jansat, D. Picurelli, K. Pelzer, K. Philippot, M. Gómez, G. Muller, P. Lecante, B. Chaudret, *New J. Chem.* **2006**, *30*, 115–122; h) D. Astruc, F. Lu, J. Ruiz Aranzaes, *Angew. Chem. Int. Ed.* **2005**, *44*, 7852–7872; i) B. Karimi, S. Abedi, J. H. Clark, V. Budarin, *Angew. Chem. Int. Ed.* **2006**, *45*, 4776–4779.

[3] a) I. W. Davies, L. Matty, D. L. Hughes, P. J. Reider, *J. Am. Chem. Soc.* **2001**, *123*, 10139–10140; b) J. A. Widegren, R. G. Finke, *J. Mol. Catal. A: Chemical* **2003**, *191*, 187–207.

[4] a) *Comprehensive Asymmetric Catalysis*, Vols. I–III, (Eds.: E. N. Jacobsen, A. Pfaltz, H. Yamamoto), Springer, Berlin, **1999**; b) *Catalytic Asymmetric Synthesis*, (Ed.: I. Ojima), 2nd edn., Wiley, New York, **2000**.

[5] a) M. Studer, H.-U. Blaser, C. Exner, *Adv. Synth. Catal.* **2003**, *345*, 45–65; b) H. Bönnemann, G. A. Braun, *Angew. Chem. Int. Ed. Engl.* **1996**, *35*, 1992–1995; c) H. Bönnemann, G. A. Braun, *Chem. Eur. J.* **1997**, *3*, 1200–1202; d) X. Zuo, H. Liu, D. Guo, X. Yang, *Tetrahedron* **1999**, *55*, 7787–7804; e) J. U. Köhler, J. S. Bradley, *Catal. Lett.* **1997**, *45*, 203–208; f) J. U. Köhler, J. S. Bradley, *Langmuir* **1998**, *14*, 2730–2735.

[6] M. Tamura, H. Fujihara, *J. Am. Chem. Soc.* **2003**, *125*, 15742–15743.

[7] a) M. T. Reetz, R. Breinbauer, K. Wanninger, *Tetrahedron Lett.* **1996**, *37*, 4499–4502; b) M. T. Reetz, E. Westermann, *Angew. Chem. Int. Ed.* **2000**, *39*, 165–168; c) M. Moreno-Mañas, R. Pleixats, S. Villarroya, *Organometallics* **2001**, *20*, 4524–4528 d) C. Rocaboy, J. A. Gladysz, *Org. Lett.* **2002**, *4*, 1993–1996; e) C. C. Cassol, A. P. Umpierre, G. Machado, S. I. Wolke, J. Dupont, *J. Am. Chem. Soc.* **2005**, *127*, 3298–3299; f) J. G. de Vries, *Dalton Trans.* **2006**, 421–429.

[8] a) C. Pan, K. Pelzer, K. Philippot, B. Chaudret, F. Dassenoy, P. Lecante, M.-J. Casanove, *J. Am. Chem. Soc.* **2001**, *123*, 7584–7593; b) K. Philippot, B. Chaudret, *C. R. Chimie* **2003**, *6*, 1019–1034; c) M. Gómez, K. Philippot, V. Collière, P. Lecante, G. Muller, B. Chaudret, *New J. Chem.* **2003**, *27*, 114–120; d) E. Ramirez, S. Jansat, K. Philippot, P. Lecante, M. Gómez, A. Masdeu, B. Chaudret, *J. Organomet. Chem.* **2004**, *689*, 4601–4610.

[9] T. Pery, K. Pelzer, G. Buntkowsky, K. Philippot, H.-H. Limbach, B. Chaudret, *ChemPhysChem.* **2005**, *6*, 605–607.

[10] a) M. Diéguez, O. Pàmies, C. Claver, *Chem. Rev.* **2004**, *104*, 3189–3215; b) M. Diéguez, O. Pàmies, A. Ruiz, Y. Diaz, S. Castillón, C. Claver, *Coord. Chem. Rev.* **2004**, *248*, 2165–2192; c) S. Castillón, C. Claver, Y. Diaz, *Chem. Soc. Rev.* **2005**, *34*, 702–713.

[11] M. Diéguez, O. Pàmies, A. Ruiz, S. Castillón, C. Claver, *Chem. Eur. J.* **2001**, *7*, 3086–3094.

[12] M. Diéguez, A. Ruiz, C. Claver, *J. Org. Chem.* **2002**, *67*, 3796–3801.

[13] S. Jansat, M. Gómez, K. Philippot, G. Muller, E. Guiu, C. Claver, S. Castillón, B. Chaudret, *J. Am. Chem. Soc.* **2004**, *126*, 1592–1593.

[14] Ligand **1**: a) G. J. H. Buisman, M. E. Martin, E. J. Vos, A. Klootwijk, P. C. J. Kamer, P. W. N. M. van Leeuwen, *Tetrahedron: Asymmetry* **1995**, *6*, 719–738; ligand **2**: b) O. Pàmies, G. Net, A. Ruiz, C. Claver, *Tetrahedron: Asymmetry* **1999**, *10*, 2007–2014; ligand **3**: c) J. E. Babin, G. T. Whiteker, *World Patent* WO93/03839, **1993**.

[15] a) P. von Matt, G. C. Lloyd-Jones, A. B. E. Minidis, A. Pfaltz, L. Macko, M. Neuburger, M. Zehnder, H. Rüegger, P. S. Pregosin, *Helv. Chim. Acta* **1995**, *78*, 265–284; b) M. Gómez, S. Jansat, G. Muller, M. A. Maestro, J. Mahía, *Organometallics* **2002**, *21*, 1077–1087.

[16] B. M. Trost, D. J. Murphy, *Organometallics* **1985**, *4*, 1143–1145.

[17] Y. Tatsuno, T. Yoshida, S. Otsuka, *Inorg. Synth.* **1990**, *28*, 342–346.

